Ir-Based Refractory Superalloys by Pulse Electric Current Sintering (PECS) Process (II Prealloyed Powder)

C. Huang, Y. Yamabe-Mitarai, and H. Harada

(Submitted 4 May 2001; in revised form 16 January 2002)

Five prealloyed powder samples prepared from binary Ir-based refractory superalloys were sintered at 1800 °C for 4 h by Pulse Electric Current Sintering (PECS). No metal loss was observed during sintering. The relative densities of the sintered specimens all exceeded 90% T.D. The best one was Ir-13% Hf with the density of 97.82% T.D. Phases detected in sintered samples were in accordance with the phase diagram as expected. Fractured surfaces were observed in two samples (Ir-13% Hf and Ir-15% Zr). Some improvements obtained by using prealloyed powders instead of elemental powders, which were investigated in the previous studies, were presented.

Keywords prealloyed powders, pulse electric current sintering

1. Introduction

A new series of materials called Ir-based refractory superalloys, which makes use of the metal Ir in the platinum group, has been investigated by Yamabe-Mitarai et al.[1] Study results show that these alloys have potential for applications at ultrahigh temperatures because of their higher melting point, good resistance to corrosion, and high-temperature strength. However, the disadvantages associated with the usual fabrication using an arc-melting process[2] must be overcome to put them into use. Powder metallurgy is an attractive approach by virtue of its advantages. The most notable advantage is that a much lower furnace temperature is required for melting. In addition, powder processing is flexible because a range of sizes and shapes can be produced from either elemental powder or prealloyed powder. In addition, the powder process can provide a finer grain and more homogeneous materials than can be achieved in most melting processes.[3]

Pulse electric current sintering (PECS), as a novel sintering method for powder densification, was tried with Ir-based refractory superalloys. In our previous work,[2] several elemental powder mixtures of Ir and one or two other metals were investigated. Some problems were experienced. First, some molten metals exited the graphite die when the temperature increased to 1800 °C during sintering because of heterogeneous melting inside the powders. This changed the composition of the samples, which we expected. Second, because of the low diffusivity of the additional element in the Ir and the fact that the powders were not completely mixed, the microstructure of the sintered sample was not homogeneous. Third, although according to the composition of the samples used the formation of a single phase was expected, second phases and even a third phase appeared after sintering, which was expected because the powders were not mixed well. Fourth, porosities, especially many small porosities, were detected in all the samples. The small porosities that remained were attributed to the use of a porous powder of Ir and Ni in the PECS process. Although porous powders have a high surface energy, sintering was not promoted, probably because of oxidation and contamination. S.H. Yoo et al.[4] also found that density did not increase steadily with a decrease in the average particle size of the ultrafine powder (2.0 ~ 0.16 μm) during plasma pressure compaction (P^2C).[4]

In the present work, prealloyed powders obtained by mechanically crushing ingots were considered instead of the elemental powders to solve the problems mentioned above. Because the melting temperature of prealloyed powder was higher than the sintering temperature of 1800 °C used here, we thought that any metal loss could be prevented during sintering. In addition, the original microstructure of prealloyed powder is believed to be uniform, and, therefore, a homogeneous structure was expected after sintering. Furthermore, prealloyed powders do not need to be blended, which had been a problem for elemental powders of Ir-based refractory superalloys with small amounts.

2. Experimental Procedure

Five samples, Ir-10 at.% Nb, Ir-15 at.% Nb, Ir-15 at.% Ti, Ir-13 at.% Hf, and Ir-15 at.% Zr, were selected with an expected single-phase fcc in Ir-16 at.% Nb and two coherent phases fcc/$L1_2$ in the others. This is the first time that fcc/$L1_2$ two-phase alloys have been investigated along with the Ir-based refractory supperalloys using the PECS process.

Ingot samples were prepared by arc melting in an Ar atmosphere and were mechanically crushed into powders. The prealloyed powders were then loaded into a graphite die and compressed by graphite punches to establish a current path.[4] To avoid contamination of the powder from graphite during sintering, graphite sheets were placed around the powders. A tablet-sized specimen was assumed after sintering. A load of about 40 MPa was applied to the powder compact, and the furnace was pumped for about 30 min to get the vacuum condition of ~0.5×10^{-2} torr. The powders were then heated to 1800 °C at a heating rate of 24 °C/s and held at that temperature for 4 h.

C. Huang, Y. Yamabe-Mitarai, and **H. Harada,** National Institute for Materials Science (NIMS), Sengen 1-2-1, Tsukuba, Ibaraki, 305-0047, Japan. Contact e-mail: huang.chen@nims.go.jp.

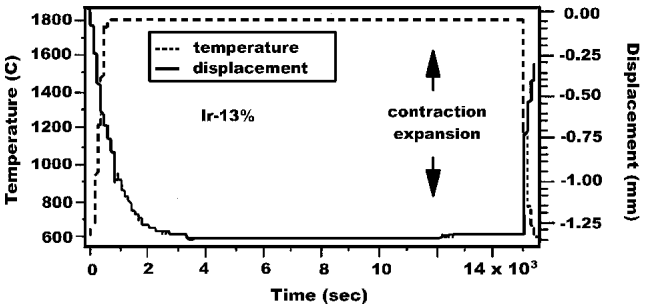

Fig. 1 Representative temperature and displacement curve during sintering of prealloyed powder samples

Table 1 Calculated and Actual Densities

Alloys (at.%)	Theoretical (max. density, g/cm³)	Actual Density (g/cm³)	Relative Density (%TD)
Ir-15% Nb	19.82	18.97	95.70
Ir-15% Ti	19.20	18.19	94.73
Ir-15% Zr	18.83	18.25	96.90
Ir-13% Hf	20.71	20.26	97.82

The displacement, temperature, and pressure of the powder compact were reported simultaneously by the computer connected to the PECS machine.

After sintering, the specimens were ground to remove the carbon contamination on the surface. The thickness, diameter, and weight of the specimens were measured by micrometer for calculating the actual density. X-ray diffraction analysis was used to determine the phase structure. The specimens were then cut, polished, and etched with a solution of 5% HCl in ethyl alcohol for optical microscope observation and SEM characterization. The phase compositions were measured by energy-dispersive analysis X-ray spectroscopy (EDX). The fracture modes were observed for Ir-13 at.% Hf and Ir-15 at.% Zr.

3. Results and Discussion

3.1 Sintering Behavior

Figure 1 shows a typical curve for temperature and displacement during sintering. Similar patterns are shown for the five specimens. Powder compacts expanded at first as the temperature increased, changed little while the temperature remained at 1800 °C, and contracted as they cooled. No metal loss was observed during sintering, and there was no sudden change on the displacement curve. Using prealloyed powders with a melting temperature >1800 °C prevented metal loss during the PECS process, which had existed in some elemental powders with one element having a low melting point.

3.2 Density and Porosity

The theoretical densities of the specimens were calculated by using a simple method of mixtures formula[2] according to nominal composition of the powders made for ingots. Actual densities were calculated and are given in Table 1 along with theoretical values. Relative densities all exceeded 90% T.D. Ir-13% Hf was the best, followed by Ir-15% Zr. The size of Ir-l0 at.% Nb could not be measured because the sample was too thin to grind off all the carbon on its surface.

Porosities were found in Ir-10% Nb, Ir-15% Nb, and Ir-15% Ti. An obvious phenomenon was that the samples had more large porosities than small porosities. An especially large number of large porosities were observed in Ir-15% Nb. Among the three samples, Ir-15% Ti was the best with fewer porosities than Ir-10% Nb and Ir-15% Nb. For Ir-15% Zr, a concentration with small porosities was observed only in the layer near the surface (Fig. 2), and no obvious porosities were detected on the inside. No porosities were observed in any part of the Ir-13%

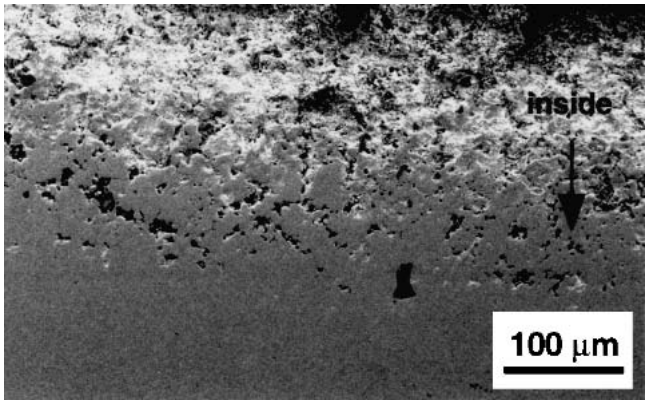

Fig. 2 Porosity morphology of Ir-15% Zr

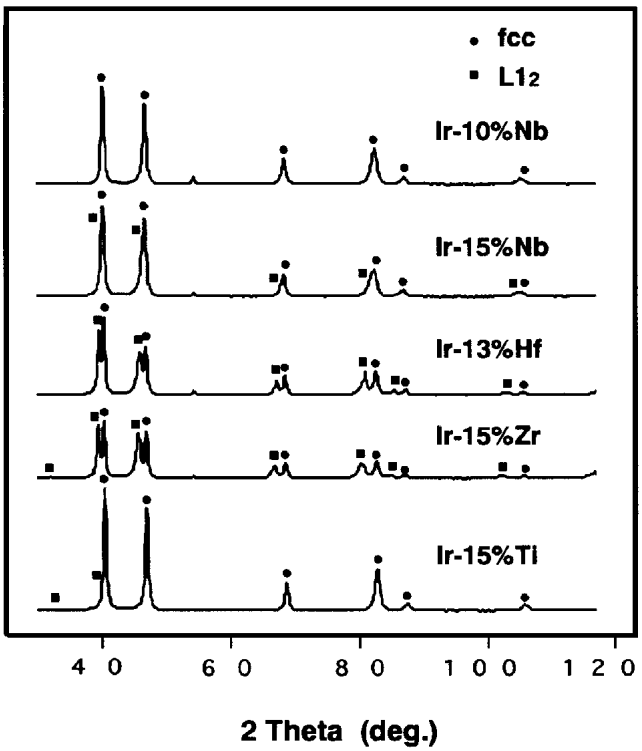

Fig. 3 XRD pattern of sintered samples

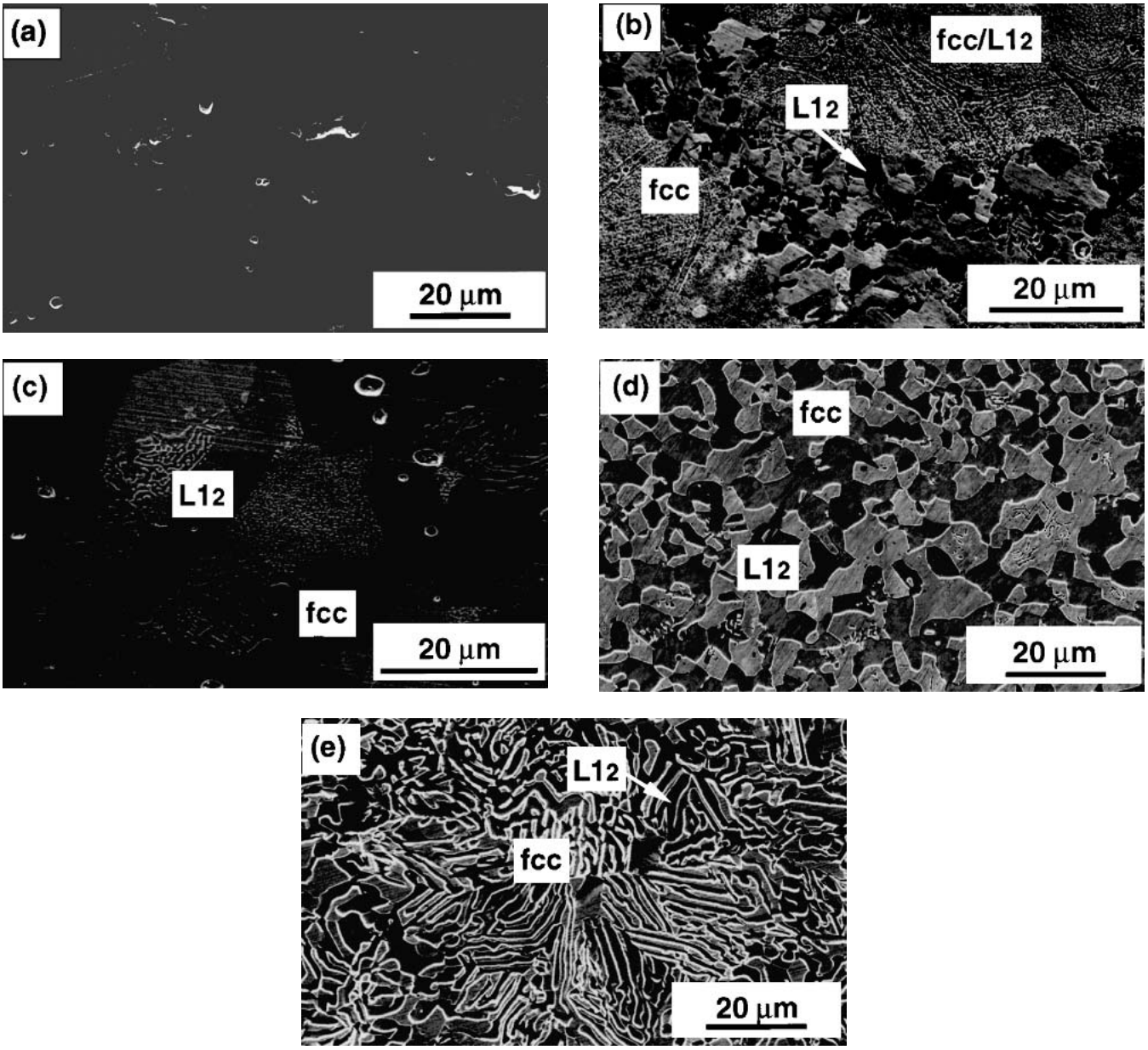

Fig. 4 Photographs of sintered samples (a) Ir-10% Nb; (b) Ir-15% Nb; (c) It-15% Ti; (d) Ir-15% Zr; and (e) Ir-13% Hf

Hf sample. According to the binary phase diagram, the melting temperatures of Ir-15% Ti, Ir-13% Hf, and Ir-15% Zr, which had fewer porosities, were <2230 °C; however, the others were >2400 °C. This finding suggested that for Ir-based prealloyed powders with large particles, a sintering temperature that increased to near the melting point was effective on elimination of porosities during the PECS process. In Ir-10% Nb, Ir-15% Nb, and Ir-15% Zr, there were fewer porosities inside the specimens than on the surface areas, which can be seen clearly in Fig. 2. This result indicates that porosities in the sample moved from the inside to the outside. This phenomenon has not been observed in samples of elemental powders. The main cause for the migration of the porosities in the prealloyed powders remains unclear. Compared with the distribution of the porosities in the samples of elemental powder, the number of small porosities here in the prealloyed powder samples decreased considerably. This also proved that the porous powder used in elemental powders in our previous study was one reason that the number of small porosities increased. This was mentioned in the previous article.[2]

3.3 Phase and Microstructure

The X-ray analysis results are shown in Fig. 3. From an X-ray pattern, one-phase fcc existed in Ir-l0 at.% Nb and fcc, $L1_2$ phases formed in the other samples, which was in accordance with the binary phase diagrams. The peaks of fcc and $L1_2$ in Ir-15% Zr and Ir-13% Hf were distinctly separated from each other because the lattice misfit between fcc and $L1_2$ of these two samples was similar (near 2%)[5] and larger than the others.

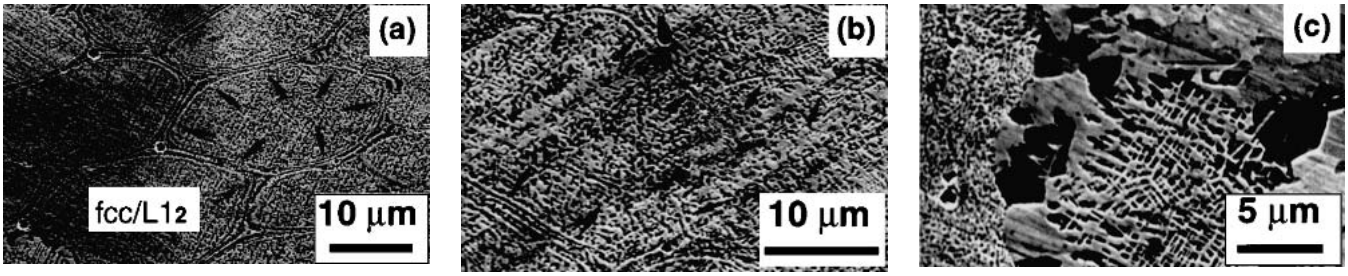

Fig. 5 Three morphologies in Ir-15% Nb

Representative micrographs of these five samples are shown in Fig. 4. A single-fcc phase existed in 10% Nb. Fcc, $L1_2$, and fcc/$L1_2$ coherent phases were found in Ir-15% Nb and Ir-15% Ti. The microstructure was heterogeneous, in two-phase alloys of Ir-15% Nb and Ir-15% Ti. Fcc and $L1_2$ coarsened structure could be seen clearly after sintering (Fig. 4b and c). This was partly due to the irregular distribution of the particle sizes in the powders and to the long period and high temperature for sintering. In Fig. 5 (a-c), three morphologies were observed in Ir-15 at.% Nb, which likely formed as a result of differences in the particulate sizes in the powder. In Fig. 5(a), a fine fcc/$L1_2$ coherent structure with an integrated grain boundary observed in some areas was considered to be an original structure, which was likely to form from one big particle. In some other areas, the grain boundary had been destroyed and had become deformed, as shown in Fig. 5(b). In many parts of the sample, some of the grains had enough driving force to grow, and the structure formed with coarsened fcc and $L1_2$, which might have come from an area of fine powder (Fig. 5c). We assumed that with suitable sintering conditions and a proper distribution of particles according to size, the homogeneous material with an fcc/$L1_2$ coherent structure could be obtained with the PECS process. We did not rule out another possibility, the irregular microstructure in the primary ingot, which might have caused the coarsening of the fcc and $L1_2$.

Ir-15% Zr and Ir-13% Hf were the best specimens observed according to porosity morphology. The microstructure also looked homogeneous in most parts of the samples (Fig. 4d and e). However, the coarsening of fcc and $L1_2$ was also very clear. The main reasons were also due to an unsatisfactory powder size, the long sintering time of 4 h, and the high sintering temperature, as mentioned above. By means of EDX, the phase with bright contrast was fcc. Figure 6 shows a remaining particle (~40 μm) that reveals the coarsening process. From the upper side to the lower side of the particle, fcc and $L1_2$ grew gradually from a fine fcc/$L1_2$ coherent structure to a coarser phase.

The phase type, grain size, and porosity distribution are summarized in Table 2.

3.4 Fracture Mode

Because the specimen was not big enough for a normal tensile test, three small and thin plate-like samples (~0.8 mm in thickness), one of Ir-15 at.% Zr, and two of Ir-13 at.% Hf, were cut by EDM and tried on tensile-test equipment by using a specially designed holder. Unfortunately, the tests failed. All the samples ruptured at the point where the sample is jointed to the holder (There was a stress concentration at the contact part of the sample and holder) and not at the neck in the middle of the sample. However, we observed the fractured surface by SEM. Photographs of the fractured surface are shown in Fig. 7. The samples were brittle. The dominant fracture mode was interboundary fracture. Obvious cracks along the boundary of Ir-13% Hf are shown in Fig. 7(a), which indicated that the boundary of Ir-13% Hf was weaker than that of Ir-15% Zr.

From the studies on ingot binary alloys of Ir-13% Hf in our group, the grain size was >100 μm, and fracture mode was intergrain boundary. In this case, the small size (<10 μm) observed here on fractured surface was not grain size but subgrain size, and fracture happened along the subgrain boundary or on the interface of phase fcc and $L1_2$. More energy is re-

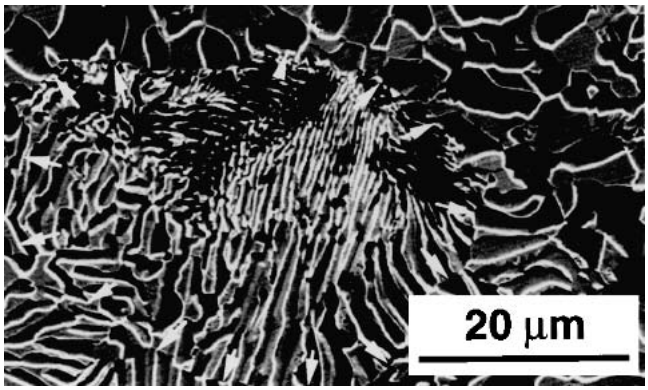

Fig. 6 A remaining particle in Ir-13% Hf

Table 2. Phase, Grain Size, and Porosity Distribution of Investigated Samples

Alloy (at.%)	Phase in Phase Diagram	Phase after Sintering	Grain Size (μm)	Porosity Distribution (b)
Ir-10% Nb	Fcc	Fcc	~20 μm	□: many; △: a few
Ir-15% Nb	Fcc,$L1_2$	Fcc,$L1_2$	~15 μm	□: more; △: a few
Ir-15% Ti	Fcc,$L1_2$	Fcc,$L1_2$	~20 μm	□: a few; △: a few
Ir-15% Zr	Fcc,$L1_2$	Fcc,$L1_2$	<10 μm (a)	□: none; △: few
Ir-13% Hf	Fcc,$L1_2$	Fcc,$L1_2$	<10 μm (a)	□: none; △: none

(a) Subgrain
(b) △, small porosity; □, big porosity

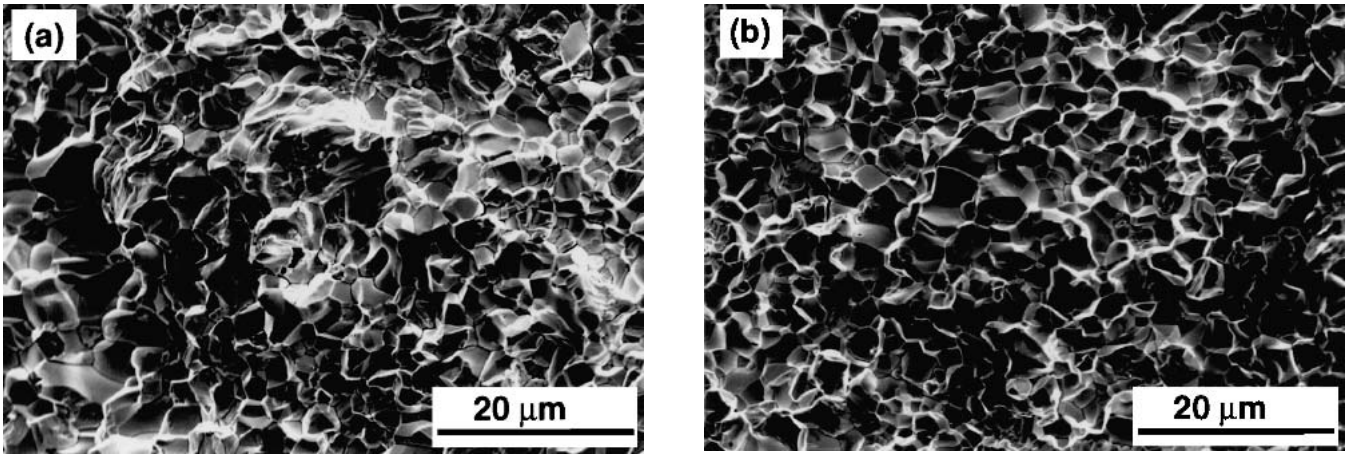

Fig. 7 Fractured surfaces of (a) Ir-13% Hf and (b) Ir-15% Zr

quired to cause this type of fracture rather than the type that occurs along the grain boundary.

3.5. PECS for Prealloyed Powder

Compared with our previous studies on elemental powder mixtures, several improvements have been achieved by using prealloyed powders. First, metal loss during sintering was prevented. From the binary phase diagram, the beginning temperatures in the formation of the liquid phase of the alloys were all >2000 °C, which meant that no liquid formed during the PECS process and that the main densification mechanism was solid-state diffusion, which stopped the metal loss. Second, the phases that formed in prealloyed powder samples were in accordance with the phase diagram. Third, although porosities still remained in Ir-10% Nb, Ir-15% Nb, and Ir-15% Ti, there were fewer small porosities than there had been when using elemental powders. No obvious porosities were detected inside Ir-15% Zr and Ir-13% Hf. Finally, a homogeneous microstructure was obtained in most parts of Ir-13% Hf and Ir-15% Zr.

We believe that the PECS process enhances the bonding of the grains by plasma generated between the particles. From the observation of the fractured surface, the PECS process really gave some improvement on fracture mode, which was intersubgrain boundary fracture instead of intergrain boundary fracture existing in ingot samples made from arc melting.

There are still a few problems to be solved. One is the coarsening of the fcc and $L1_2$ phases in the two-phase samples, which is mainly attributable to the long sintering time and high sintering temperature used. Moreover, compared with the ingot samples, it seemed that the samples became coarse more quickly during sintering than they would have during a normal heat treatment. The fcc/$L1_2$ two-phase coherent structure was the key to high-temperature, high-strength materials, which was expected in Ir-based binary alloys. Suitable powder and sintering condition will be investigated further to limit the coarsening of fcc and $L1_2$. Another problem is the heterogeneous microstructure, which can most likely be attributed to the powder. The powders were irregular in the distribution of the particulates because they were manufactured by mechanically crashing. The differences of the particle size caused the irregular grain growth during sintering. In addition, the shape of the powder created by this preparation method was unsatisfactory. Finally, porosities still existed in some samples. Higher sintering temperatures could possibly lead to the elimination of the porosity.

4. Summary

- Ir-based refractory superalloys with a relative density >90% T.D. were obtained from prealloyed powders by using the PECS method. Ir-13% Hf was the best sample with 97.82% T.D.
- An fcc phase was observed in Ir-10% Nb, and fcc, $L1_2$ phase was observed in the others, which was in accord with the binary phase diagram.
- Metal loss was prevented by using prealloyed powders.
- The fracture mode for Ir-13% Hf and Ir-15% Zr was intersubgrain boundary fracture. Some enhancements in the grain boundary had been achieved by the PECS process.
- The PECS process has some potential for the development of Ir-based refractory superalloys. At this point, further investigations are still required.

Acknowledgments

The authors thank Dr. S. Nishimura and Dr. N. Hirosaki for supplying PECS equipment, and Dr. Y. Gu for his helpful discussions in our research.

References

1. Y. Yamabe-Mitarai, Y. Ro, T. Maruko and H. Harada, "Ir-Base Refractory Superalloys for Ultra-High Temperature," *Metall. Mater. Trans. A, 1998, 29A,* pp. 537-49.
2. C. Huang, Y. Tamabe-Mitarai, and H. Harada, "Ir-based Refractory Superalloys by Pulse Electric Current Sintering (PECS) Process (I Elemental Powder)" *J. Mater. Eng. Performance,* 2001, *10,* pp. 629-34.
3. D.E. Alman, N.S. Stoloff, and M. Otsuki, "Powder Processing and Mechanical Properties of Intermetallic Matrix Composites," JIMIS-6, Sendai, Japan, pp. 891-99.
4. S.H. Yoo, T.S. Sudarshan, K. Sethuram, G. Subhash, and R.J. Dowding, "Dynamic Compression Behaviour of Tunsten Powders Consolidated by Plasma Pressure Compaction," *Powder Metall.,* 1999, *42*(2), pp. 181-82.
5. Y. Yamabe-Mitarai, X. Yu, Y. Gu, Y. Ro, S. Nakazawa, T. Maruko, and H. Harada, "High Temperature Strength of Ir-Base Refractory Superalloys," *Key Eng. Mater.,* 2000, *171-174,* pp. 625-32.